

Alfa- Bismuth(III)oxide catalyzed Biginelli reactions using experimentally designed optimized condition

Marzie Sabaghian^a, Mahdi Behzad^{a*}, Hamideh Samari Jahromi^b

^aDepartment of Chemistry, Semnan University, Semnan 35351-19111, Iran

^bResearch Institute of Petroleum Industry (RIPI), Environment and Biotechnology Division, West Blvd., Azadi Sports Complex, P.O. Box 14665-1998, Tehran, Iran

ARTICLE INFO

Article history:

Received 13 November 2015

Accepted 27 December 2015

Available online 20 January 2015

Keywords:

Bi₂O₃

Hydrothermal method

Experimental design

Biginelli

ABSTRACT

α -Bi₂O₃ was synthesized via a hydrothermal method at 180 °C for 12 h in 1 (S₁) and 2 (S₂) M KOH aqueous solutions, using Bi(NO₃)₃·5H₂O as raw material. The synthesized material was characterized by X-ray powder diffraction (XRPD) technique. The XRPD results indicated that by using 1M KOH aqueous solution, α -Bi₂O₃ was obtained with small fractions of β -Bi₂O₃, while 2M KOH solution resulted in pure α -Bi₂O₃. The α -Bi₂O₃ was crystallized in a monoclinic crystal structure with space group of P2₁/c. The size and morphology of the synthesized material was studied by field emission scanning electron microscopy (FE-SEM). The FE-SEM images showed that the obtained material had multigonal structures in micron dimensions. The synthesized material was tested as catalyst in Biginelli reactions and excellent performance was achieved in the optimized conditions. Experimental design was used to obtain optimized reaction conditions. Also, the optical properties of the obtained material were studied by ultraviolet visible (UV-Vis) diffuse reflectance spectrum (DRS).

1. Introduction

Bi₂O₃ is an important semiconductor with several main crystallographic polymorphs denoted by alpha (monoclinic), beta (tetragonal), gamma (cubic), delta (cubic), omega (triclinic) and epsilon (orthorhombic) crystal phases. Under normal atmospheric conditions α - and δ -Bi₂O₃ are the stable phases at room temperature, while β -, γ -, ω and ϵ -Bi₂O₃ phases are high-temperature metastable phases [1-4]. In the last years, Bi₂O₃ has gained noticeable attention due to its good absorption capacity [5], dielectric permittivity, considerable photoconductivity and photoluminescence, and high refractive index [6]. Because of these properties, Bi₂O₃ can be used in piezo-optic materials [7], superconductor ceramic glass manufacturing [8], solar cells [9], sensor optical coatings [10],

oxide-ion conductors[11], bacteria inactivation[12], photovoltaic cells [13], gas sensing [14], fuelcells [15], and photocatalysis[16]. Until now, several methods such as solvothermal[17-19], sol-gel [20-22], chemical vapor deposition (CVD) [23], reactive sputtering deposition [24], thermolysis [25-26], and SPRT method [4] have been reported for the synthesis of Bi₂O₃. In this work, a simple hydrothermal method was employed for the synthesis of α -Bi₂O₃, at 180 °C for 12h using Bi(NO₃)₃·5H₂O and KOH as raw materials. The obtained material was characterized by XRPD and FE-SEM techniques and tested as catalyst in Biginelli reactions for the synthesis of 3,4-dihydropyrimidin-2-(1H)-ones (DHPMs). Several parameters including reaction time, temperature and the amount of the catalyst

* Corresponding Author:

E-mail Address: mbehzad@semnan.ac.ir

were optimized by experimental design method using full factorial design coupled to response surface methodology (RSM) [27]. 3,4-Dihydropyrimidin-2-(1H)-ones (DHPMs) are important materials in organic chemistry and have found applications in biochemistry [28-29] and biology [30]. Various catalysts have been used for the synthesis of these materials. In most of the previously reported catalytic methods for such type of reaction, a one-at-a-time approach is applied [31-33]. In one-at-a-time method, one parameter is varied while the other parameters are kept constant to find the optimum amount of the variable. It is known that the reaction parameters are not independent of each other, so it could have been better to optimize the catalytic reaction conditions simultaneously. In the present research, experimental design method was used to find the optimized reaction condition for α -Bi₂O₃ catalyzed Biginelli reactions. Excellent performance was achieved in the optimized conditions.

2. Experimental

2.1. General remarks

All chemicals including Bi(NO₃)₃·5H₂O and KOH were of analytical grade and were obtained from Merck Company, Germany and used without further purification. Phase identifications were performed on a powder X-ray diffractometer D5000 (Siemens AG, Munich, Germany) using CuK_α radiation. The morphology of the obtained materials was examined by a field emission scanning electron microscope (Hitachi FE-SEM model S-4160). The purity of the DHPMs was checked by thin layer chromatography (TLC) on glass plates coated with silica gel 60 F254 using n-hexane/ethyl acetate mixture as mobile phase. The UV-Vis diffuse reflectance spectra of the samples were recorded using an Avantes Spectrometer model Avaspec-2048-TEC. Cell parameter refinement was performed by celref software version 3 (Laboratoire des Matériaux et du Génie Physique de l'École Supérieure de Physique de Grenoble).

2.2. Hydrothermal synthesis of α -Bi₂O₃

In a typical experiment for preparing S₁, 1.00 g (2.06 mmol) of Bi(NO₃)₃·5H₂O (M_w = 485.07 g mol⁻¹) was added to 50 mL of hot aqueous

solution (80 °C) of 1M KOH in a baker. The resulting solution was magnetically stirred for 15 min and then transferred in to a 100-mL teflon lined stainless steel autoclave. The autoclave was sealed and heated at 180 °C for 12 h. When the reaction was completed, the reactor was immediately cooled to room temperature by immersing in water. The prepared powder was washed with distilled water and dried at 120 °C for 20 min under normal atmospheric conditions and the yellow powder was collected by filtration. The yield was 0.42 g (87%). S₂ was prepared following similar procedure except the reaction was performed in 2M KOH solution and 0.45 g (93%) of the product was obtained.

2.3. General procedure for the synthesis of DHPMs

In a typical experiment, a mixture of aldehyde (1 mmol), ethyl acetoacetate (1 mmol), urea (1.2 mmol) and α -Bi₂O₃ (S₂) as catalyst were placed in a round-bottom flask under solvent free conditions. The suspension was stirred at 120 °C while the reaction progress was being monitored by thin layer chromatography (TLC) [6:4=hexane:ethylacetate]. After completion of the reaction, the solid product was washed with deionized water to separate the unreacted raw materials. The precipitated solid was then collected and dissolved in ethanol to separate the solid catalyst. The filtrate was evaporated to dryness by a rotary evaporator to afford the crude product which was then recrystallized in ethanol to afford crystals of the pure product.

3. Results and discussion

3.1. Characterization

Figure 1(a, b) shows the XRPD patterns of S₁ and S₂, respectively. The XRPD pattern of S₁ consists of a mixture of a predominant α -Bi₂O₃ (JCPDS file No. 41-1449) and a minor β -Bi₂O₃ (JCPDS file No 27-0050). The peaks at the 2 θ (hkl) values at 27.1(111), 27.5(120), 33.3(040), 46.3(041), 52.5(321), 61.5(241) are characteristic of the monoclinic α -Bi₂O₃ phase with the space group *P*2₁/*c*. The α -Bi₂O₃ crystal lattice parameters were found to be *a*=5.8499Å, *b*=8.1698Å, and *c*=7.5123Å with $\alpha = \gamma = 90^\circ, \beta = 112.99^\circ$. The β -Bi₂O₃ structure was detected with a space group of

$P4_2/c$. The β - Bi_2O_3 lattice parameters were found as $a=b=7.742\text{\AA}$, and $c=5.631\text{\AA}$ with $\alpha = \gamma = \beta = 90^\circ$. On the other hand, all the sharp and strong diffraction peaks in figure 1b for S_2

can be indexed to the monoclinic phase of α - Bi_2O_3 (JCPDS file No. 41-1449, space group $P2_1/c$), indicative of the excellent purity of α - Bi_2O_3 [34].

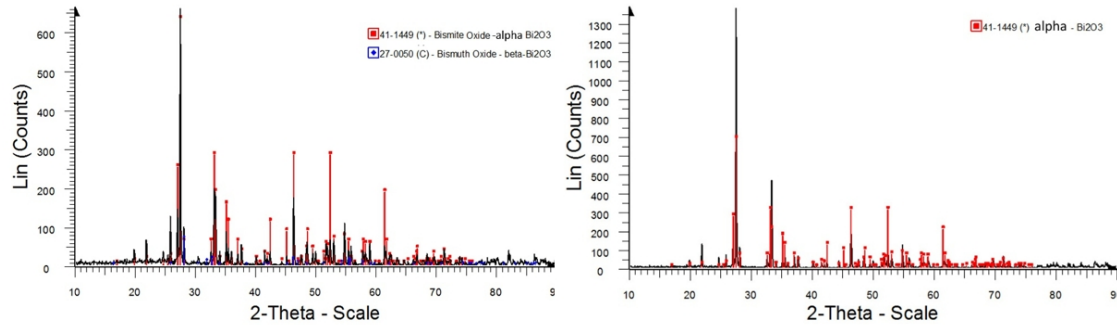


Fig. 1. XRPD patterns of (left) S_1 and (right) S_2 .

Figures 2a and b show the FE-SEM images of S_1 and S_2 , respectively. Figure 2a shows that the obtained material has a multigonal crystalline morphology with micron dimensions. It was found that the width of the particle is about $2\ \mu\text{m}$. Besides, it is clear that there are some particles on the surface of the

material. The diameter of the particles is about $600 - 700\ \text{nm}$. Figure 2b shows that with changing the reaction route, morphology of the obtained material was nearly unchanged. However, it seems that the width of the material increased to about $3\ \mu\text{m}$.

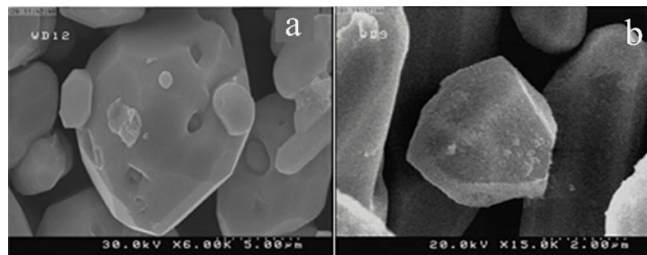


Fig. 2. FE-SEM images of S_1 and S_2 .

The direct optical band gap for pure Bi_2O_3 , obtained from UV-Vis DRS spectrum is shown in figure 3. To calculate the optical band gap, we changed transmittance data to absorption ones using $A = -\log(T/100)$ formula, where A is absorption and T is transmittance. According to the results of Pascual et al. [35], the relation between the

absorption coefficient and incident photon energy can be written as $(\alpha h\nu)^2 = A(h\nu - E_g)$, where A and E_g are constant and direct band gap energy, respectively. Band gap energy was evaluated by extrapolating the linear part of the curve to the energy axis. It was found that the band gap of Bi_2O_3 was about $4.2\ \text{eV}$.

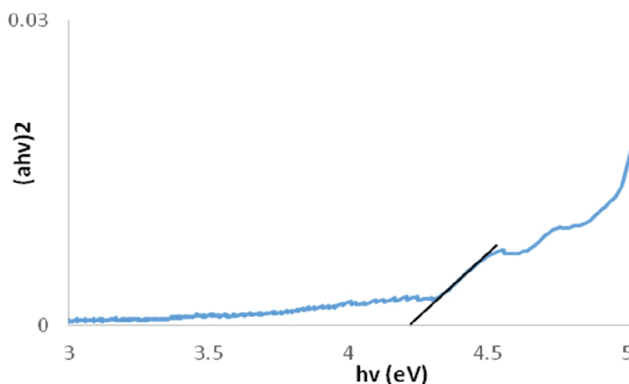


Fig. 3. The Plot of $(ahv)^2$ versus hv (eV) for S_2 .

3.2. Catalytic studies

3.2.1. Central composite design and optimal condition in Biginelli reactions

Central composite design (CCD) is one of the most popular methods in [response surface methodology \(RSM\)](#) for building a second order (quadratic) model for the [response variables](#) without any need to use a complete five-level [factorial experiment](#)[36-37]. A CCD consists of a factorial design with center points that is augmented with a group of 'star points' that can estimate curvatures in the response. The star points hold new extremes for the low and high settings for all factors. The number of experiments (N) required for conducting of CCD is defined by equation 1:

$$N = 2^k + 2k + c_0 \quad (1)$$

Where k is the number of factors. There are 2^k factorial points, $2 \times k$ star points and c_0 is the number of central point [35-36]. In our study, in Biginelli reaction, three factors, i.e. the amount of the catalyst (X_1), temperature (X_2) and time of the reaction (X_3) were designed as shown in Table 1. These factors were coded in five levels of - a, -1, 0, +1, + a for the lowest, low, middle, high and the highest values, respectively. Twenty experiments were required in this design including six center points and they were performed randomly in three days. All the

experiments and the design have been reported in Table 2.

Table 1. Factors and levels used in the CCD design.

Factors	Symbol	Coded Levels				
		- a	-1	0	1	a
The amount of the catalyst (g)	X_1	0.005	0.014	0.028	0.042	0.050
Temperature ($^{\circ}C$)	X_2	40	56	80	104	120
Time (min)	X_3	10	24	80	65	80

Table 2. Design matrix and responses for the CCD design.

Catalyst amount (g)	Temp ($^{\circ}C$)	Time (min)	Yield (%)
day1			
0.041	56	66	32
0.014	56	24	13
0.028	80	45	20
0.014	104	66	84
0.041	104	24	63
0.028	80	45	18

day2			
0.041	56	24	12
0.014	56	66	10
0.028	80	45	23
0.028	80	45	28
0.014	104	24	36
0.041	104	66	85
day3			
0.028	120	45	98
0.028	80	45	23
0.050	80	45	38
0.028	80	10	7
0.028	80	80	25
0.028	80	45	18
0.028	40	45	65
0.005	80	45	24

There is a theoretical function in which the relation between factors and response can be defined. This relation leads to the reproducibility in the phenomenon under study to be able to experiment with it and to present an accurate interpretation of the variation in data. RSM is a mathematical and statistical method, which can analyze experimental design data based on an empirical model [27]. It uses the analysis of variance (ANOVA) [38] to verify the adequacy of the applied model. The observed data of the factorial design (Table 2) were fitted to a quadratic response model. The analysis has been done based on the coded values of the factors. Also the fifth data were outlier and omitted. Equation 2 shows the relation between the factors and the yield of the reaction, Y%, based on the quadratic model:

$$Y\% = 17.76 + 5.36 X_1 + 18.74 X_2 + 8.59 X_3 + 6.43X_2X_3 + 3.71X_1^2 + 21.61 X_2^2 \quad (2)$$

X_1 , X_2 and X_3 are the same as introduced in Table 1. This equation shows that not only the main factors X_1 , X_2 and X_3 are important, but also the interaction effects of time and temperature (X_2 and X_3 , respectively) and the square of factors X_1 and X_2 are significant. So, in the optimization of the reaction conditions, all of these parameters must be considered. It is worth noticing that the more the value of the parameters, the more the effect. For example,

the effect of the square of the catalyst is the highest one, and then the temperature shows the highest effect among the others.

The ANOVA results reported in Table 3 showed that the p-value of the regression was smaller than 0.05, which was the indicator of the significant model at a high confidence level (95%) [27]. The p-value probability of lack of fit was more than 0.05, which verified the significance of the models. Besides, the coefficients of determination (the R-square, adjusted-R-square) were used to express the quality of fit of polynomial model equation. In this case, R^2 of variation fitting for Y% 0.9257 indicated a high degree of correlation between the response and the independent factors. Also, the adjusted regression coefficient (R^2 -adj = 0.8812) indicated the significance of the proposed model. To illustrate the effects in the above models, the three-dimensional (3D) response surfaces plot of the response (using equation (1) when the amount of the catalyst was fixed at center level (0.03 g) and the other two were allowed to vary) is shown in figure 4. The curvature of the plot is an indicator of the presence of the interaction between the factors, a fact which means that the factors may affect the response interactively and not independently. So, their combined effect is different from the straight addition of the effects.

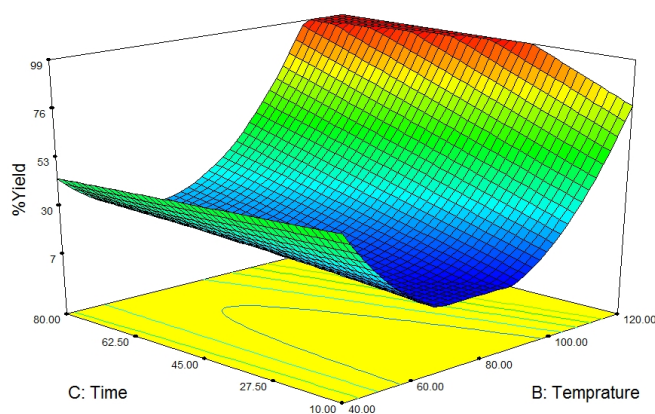


Fig. 4. Response surface plots of Y% vs. temperature and time at the center level of the catalyst (0.03g).

Table 3. Analysis of variance for suggested quadratic model.

Source	DF	SS	F	P
Block	2	85.31		
Regression	6	13144.87	20.77	<0.0001
Residual error	10	1054.75		
Lack-of-fit	8	1040.58	18.36	0.0527
Pure error	2	14.17		
Total	18	14284.93		

3.2.2. Synthesis of DHPMs

The goal of the optimization was to maximize the yield of the reaction corresponded to the condition of experiment in which the above equation was maximized. The results showed that 0.028 g of the catalyst, 120 °C reaction

temperature, and 45 min reaction time were the optimum parameters for the synthesis of DHPMs (Table 2). The optimized parameters were used for the synthesis of other derivatives and the results are collected in Table 4. Figure 5 shows a summary of the reaction pathway.

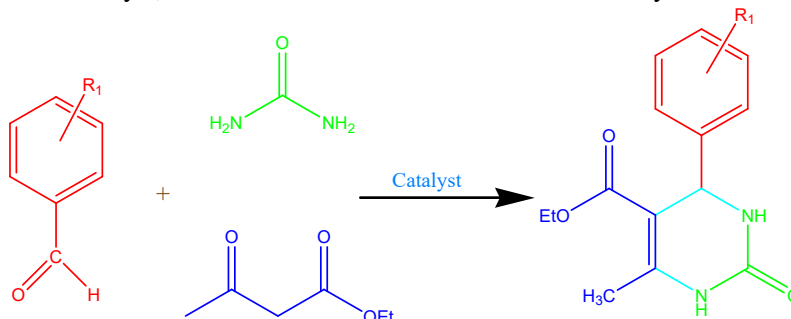


Fig. 5. Schematic representation of the reaction pathway for the synthesis of DHPMs.

Table 4. Biginelli reactions using ethyl acetoacetate and urea with different benzaldehyde derivatives.

R ₁	Conversion (%)
H	98
4- Cl	98
4- Br	85
3-OH	70
4-OH	95
3,4-OH	91
2- Cl	60
3-NO ₂	88

Table 5 shows the catalytic efficiency of the synthesized Bi_2O_3 nanomaterials compared with the starting material $\text{Bi}(\text{NO}_3)_3 \cdot 5\text{H}_2\text{O}$. The optimized conditions from the previous section

were used. As can be seen from Table 5, Bi_2O_3 was a more efficient catalyst compared to the starting material.

Table 5. Comparison study of the catalytic ability of the synthesized Bi_2O_3 with raw material.

Catalyst	Reagents	Time (min)	Yield
Bi_2O_3	Benzaldehyde	45	98.3
$\text{Bi}(\text{NO}_3)_3 \cdot 5\text{H}_2\text{O}$	Benzaldehyde	45	82.6

To show the merit of the present work in comparison with the results reported in the literature, we compared Bi_2O_3 nanocatalyst results with reported catalysts in the synthesis

of DHPMs (Table 6). It is clear that Bi_2O_3 shows greater activity compared to some other heterogeneous catalysts.

Table 6. Comparison study of the catalytic ability of the synthesized Bi_2O_3 with other catalysts.

Catalyst	R_1	Catalyst amount	Condition	Yield %	Time (min)	Ref.
Bi_2O_3	H	6 mol%	solvent-free, 120 °C	98	45	This work
	4- Cl			98		
	2-Cl			60		
$\text{Bi}_2\text{O}_3/\text{ZrO}_2$	H	20 mol%	solvent-free, 80-85 °C	85	120	[39]
	4- Cl			85		
	2- Cl			82		
$\text{ZrO}_2\text{-Al}_2\text{O}_3\text{-Fe}_3\text{O}_4$	H	0.05 g	Ethanol, reflux, 140 °C	82	300	[40]
	4- Cl			66		
	2- Cl			40		
$\text{Mo}/\gamma\text{-Al}_2\text{O}_3$	H	0.3 g	solvent-free at 100 °C	80	60	[41]
ZnO	H	25 mol%	solvent-free at 90 °C	92	50	[42]
	4- Cl			95		

4. Conclusion

In summary, pure $\alpha\text{-Bi}_2\text{O}_3$ was prepared via a facile hydrothermal method. The XRPD data showed that with increasing the basic solution concentration from 1M to 2M of KOH, the $\alpha\text{-Bi}_2\text{O}_3$ crystal purity improved and the $\beta\text{-Bi}_2\text{O}_3$ impurity eliminated. FE-SEM images showed that the obtained material had multigonal crystalline morphology with micron dimensions. The obtained $\alpha\text{-Bi}_2\text{O}_3$ (S_2) was used as catalyst in Biginelli reaction for the synthesis of DHPM derivatives. Optimized conditions were obtained by experimental design method. It was found that the optimum conditions were 120 °C as the reaction temperature, 0.028 g of S_2 for 45 min under solvent free condition. The highest efficiency of the catalyst was achieved for the synthesis of benzaldehyde derivative in the optimum conditions.

5. Acknowledgement

We gratefully acknowledge Dr. Seyyedeh Maryam Sajjadi and ShahinKhademinia for their helps and comments.

References

- [1] N. Cornei, N. Tancret, F. Abraham, O. Mentre'. "New $\epsilon\text{-Bi}_2\text{O}_3$ Metastable Polymorph", *Inorg. Chem.*, Vol. 45, 2006, pp. 4886-4888.
- [2] S. Cao, P. Zhou, J. Yu, "Recent advances in visible light Bi-based photocatalysts", *Chinese. J. Catal.*, Vol. 35, 2014, pp. 989-1007.
- [3] F. Schröder, N. Bagdassarov, F. Ritter, L. Bayarjargal, "Temperature dependence of Bi_2O_3 structural parameters close to the $\alpha\text{-}\delta$ phase transition", *Phase Transitions*. Vol. 83, 2010, pp. 311-325.

- [4] M. Prekajski, A. Kremenović, B. Babić, M. Rosić, B. Matović, A. Radosavljević-Mihajlović, M. Radović. "Room-temperature synthesis of nanometric α -Bi₂O₃", *Materials Letters.*, Vol. 64, 2010, pp. 2247–2250.
- [5] K. Brezesinski, R. Ostermann, P. Hartmann, J. Perlich, T. Brezesinski, "Exceptional photocatalytic activity of ordered mesoporous β -Bi₂O₃ thin films and electrospun nanofiber mats," *Chem. Mater.*, 22, 2010, pp. 3079-3085.
- [6] J.-y. Xia, M.-T. Tang, C. Cui, S.-M. Jin, Y.-M. Chen, "Preparation of α -Bi₂O₃ from bismuth powders through low-temperature oxidation," *Trans. Nonferrous. Met. Soc. China.*, Vol. 22, 2012, pp. 2289-2294.
- [7] A. Feldman, W. S. Brower Jr, D. Horowitz, "Optical activity and Faraday rotation in bismuth oxide compounds," *App. Phys. Lett.*, Vol. 16, 1970, pp. 201-202.
- [8] A. Pan, A. Ghosh, "A new family of lead–bismuthate glass with a large transmitting window," *J. Non. Cryst. Solids.*, Vol. 271, 2000, pp. 157-161.
- [9] E. Y. Wang, K. A. Pandelišev, "The effect of chemical surface treatments on non-native (Bi₂O₃) GaAs metal-insulator-semiconductor solar cells," *J. Appl. Phys.*, Vol. 52, 1981, pp. 4818-4820.
- [10] M. Schuisky, A. Hårsta, "Epitaxial growth of Bi₂O_{2.33} by halide Cvd," *Chem. Vapor. Depos.*, Vol. 2, 1996, pp. 235-238.
- [11] S. Beg, S. Haneef, N. A. Al-Areqi, "Study of electrical conductivity and phase transition in Bi₂O₃–V₂O₅ system," *Phase Transitions.*, Vol. 83, 2010, pp. 1114-1125.
- [12] F. Qin, H. Zhao, G. Li, H. Yang, J. Li, R. Wang, Y. Liu, J. Hu, H. Sun, R. Chen, "Size-tunable fabrication of multifunctional Bi₂O₃ porous nanospheres for photocatalysis, bacteria inactivation and template-synthesis," *Nanoscale.*, Vol. 6, 2014, pp. 5402-5409.
- [13] A. Cabot, A. Marsal, J. Arbiol, J. Morante, "Bi₂O₃ as a selective sensing material for NO detection," *Sensor. Actuat B:Chem.*, Vol. 99, 2004, pp. 74-89.
- [14] X. Gou, R. Li, G. Wang, Z. Chen, D. Wexler, "Room-temperature solution synthesis of Bi₂O₃ nanowires for gas sensing application," *Nanotechnol.*, Vol. 20, 2009, pp. 1-5.
- [15] K. T. Lee, A. A. Lidie, S. Y. Jeon, G. T. Hitz, S. J. Song, E. D. Wachsman, "Highly functional nano-scale stabilized bismuth oxides via reverse strike co-precipitation for solid oxide fuel cells," *J. Mater. Chem:A.*, Vol. 1, 2013, pp. 6199-6207.
- [16] M. Schlesinger, S. Schulze, M. Hietschold, M. Mehring, "Metastable β -Bi₂O₃ nanoparticles with high photocatalytic activity from polynuclear bismuth oxido clusters," *Dalton. Trans.*, Vol. 42, 2013, pp. 1047-1056.
- [17] Z. Yu, J. Zhang, H. Zhang, Y. Shen, A. Xie, F. Huang, S. Li, "Facile solvothermal synthesis of porous Bi₂O₃ microsphere and their photocatalytic performance under visible light," *Micro. Nano. Lett.*, Vol. 7, 2012, pp. 814-817.
- [18] J. Wang, J. Liu, B. Wang, L. Zhu, J. Hu, H. Xu, "Fabrication of alpha-Bi₂O₃ Microrods by Solvothermal Method and Their Photocatalytic Performance," *Chem. Lett.*, Vol. 43, 2014, pp. 547-549.
- [19] X. Luan, J. Jiang, Q. Yang, M. Chen, M. Zhang, L. Li, "Facile synthesis of bismuth oxide nanoparticles by a hydrolysis solvothermal route and their visible light photocatalytic activity," *Environ. Eng. Manag. J.*, Vol. 14, 2015, pp. 703-707.
- [20] J. Zhang Li, J. Bo Zhong, J. Zeng, F. Mei Feng, J. Jin He, "Improved photocatalytic activity of dysprosium-doped Bi₂O₃ prepared by sol–gel method," *Mat. Sci. Semicon. Proc.*, Vol. 16, 2013, pp. 379-384.
- [21] H. Weidong, Q. Wei, W. Xiaohong, N. Hailong, "Thin bismuth oxide films prepared through the sol–gel method," *Mater. Lett.*, Vol. 61, 2007, pp. 4100-4102.
- [22] M. Mallahi, A. Shokuhfar, M. Vaezi, A. Esmaeilirad, V. Mazinani, "Synthesis and characterization of Bismuth oxide nanoparticles via sol-gel method," *Am. J. Eng. Res.*, Vol. 3, 2014, pp. 162-165.
- [23] T. Takeyama, N. Takahashi, T. Nakamura, S. Ito, "Growth of the Bi₂O₃ thin films under atmospheric pressure by

- means of halide CVD," *J. Phys. Chem. Solids.*, Vol. 65, 2004, pp. 1349-1352.
- [24] H. Fan, X. Teng, S. Pan, C. Ye, G. Li, L. Zhang, "Optical properties of δ -Bi₂O₃ thin films grown by reactive sputtering," *App. Phys. Lett.*, Vol. 87, 2005, pp. 1-3.
- [25] M. Sadeghi Roodsari, B. Shaabani, B. Mirtamizdoust, M. Dusek, K. Fejfarova, "Sonochemical Synthesis of Bismuth (III) Nano Coordination Compound and Direct Synthesis of Bi₂O₃ Nanoparticles from a Bismuth (III) Nano Coordination Compound Precursor" *J. Inorg. Organomet. Polym.*, Vol. 25, 2015, pp. 1226-1232.
- [26] Y. Hanifehpour, B. Mirtamizdoust, M. Hatami, B. Khomami, S.W. Joo, *J. Mol. Struc.* Vol.5, 2015, pp. 43-48.
- [27] G. E. Box, N. R. Draper, "Empirical model-building and response surfaces: Wiley Series in probability and mathematical statistics," *S. Prob. Math. Stat.*, (1987), ISBN 0471810339, 9780471810339.
- [28] D. Song, R. Wang, Y. Chen, S. Zhang, C. Liu, G. Luo, "Copper (II) trifluoroacetate catalyzed synthesis of 3, 4-dihydropyrimidin-2 (1H)-ones under solvent-free conditions," *Reac. Kinet. Mech. Cat. Lett.*, Vol. 95, 2008, pp. 381-385.
- [29] A. Dubey, B. G. Mishra, D. Sachdev, M. Sowmiya, "Heterogeneous liquid phase synthesis of 3, 4-dihydropyrimidine-2 (1H)-ones using aluminated mesoporous silica," *Reac. Kinet. Mech. Cat. Lett.*, Vol. 93, 2008, pp. 149-155.
- [30] F. Xu, J. J. Wang, Y. P. Tian, "New Procedure for One-Pot Synthesis of 3, 4-Dihydropyrimidin-2 (1 H)-ones by Biginelli Reaction," *Synth. Commun.*, Vol. 38, 2008, pp. 1299-1310.
- [31] Q. Song, X. An, F. Che, T. Shen, "Novel and Efficient Synthesis of DHPMs Catalyzed by di-DACH-Pyridylamide Ligands," *J. Heterocyclic. Chem.*, Vol. 52, 2014, pp.1496-1502.
- [32] Y. Moussaouia, R. B. Salemb, "Synthesis of 3,4-Dihydropyrimidinones via Phase Transfer Catalysis," *J. Heterocyclic. Chem.*, Vol. 50, 2013, pp.1209-1212.
- [33] S. Tu, F. Fang, S. Zhu, T. Li, X. Zhang, Q. Zhuang, "A new Biginelli reaction procedure using potassium hydrogen sulfate as the promoter for an efficient synthesis of 3, 4-dihydropyrimidin-2 (1H)-one," *Synlett.*, Vol. 15, 2004, pp. 537-539.
- [34] Q. Yang, Y. Li, Q. Yin, P. Wang, Y.-B. Cheng, "Hydrothermal synthesis of bismuth oxide needles," *Mater Lett.*, Vol. 55, 2002, pp. 46-49.
- [35] J. Pascual, J. Camassel, M. Mathieu, "Fine structure in the intrinsic absorption edge of TiO₂," *Phys. Rev. B: Solid State.*, Vol. 18, 1978, pp. 5606-5614.
- [36] R. Myer, D.C. Montgomery, "Response surface methodology: process and product optimization using designed experiment, 3rd Ed," John Wiley and Sons: New York., 2002, pp. 343-350.
- [37] E.D. Morgan, "Chemometrics: Experimental Design," Wiley., 1995.
- [38] R. Tauler, B. Walczak, S. D. Brown, "Comprehensive chemometrics: chemical and biochemical data analysis," Elsevier., Vol. 1, 2009, ISBN: 978-0-444-52701-1.
- [39] S. Battu, V. C. Guguloth, G. Raju, M. Basude, "Efficient, stable and reusable Bi₂O₃/ZrO₂ catalyzed one-pot synthesis of 3, 4-dihydropyrimidin-2 (1H)-ones under solvent-free conditions," *Int. J. Chem. Anal. Sci.*, Vol. 5, 2014.
- [40] A. Wang, X. Liu, Z. Su, H. Jing, "New magnetic nanocomposites of ZrO₂-Al₂O₃-Fe₃O₄ as green solid acid catalysts in organic reactions," *Catal. Sci. Technol.*, Vol. 4, 2014, pp. 71-80.
- [41] S. L. Jain, V. Prasad, B. Sain, "Alumina supported MoO₃: An efficient and reusable heterogeneous catalyst for synthesis of 3, 4-dihydropyrimidine-2 (1H)-ones under solvent free conditions," *Catal. Commun.*, Vol. 9, 2008, pp. 499-503.
- [42] K. Pourshamsian, "ZnO-NPs as an efficient reusable heterogeneous catalyst for synthesis of 1, 4-Dihydropyrimidine derivatives in solvent-free conditions," *Int. J. Nano. Dimens.*, Vol. 6, 2015, pp. 99-104.